

Density Functional Theory for the Nonspecific Binding of Salt to Polyelectrolytes: Thermodynamic Properties

Chandra N. Patra and Arun Yethiraj

Department of Chemistry, University of Wisconsin, Madison, Wisconsin 53706 USA

ABSTRACT The thermodynamics of the nonspecific binding of salt to a polyelectrolyte molecule is studied using a density functional approach. The polyelectrolyte molecule is modeled as an infinite, inflexible, and impenetrable charged cylinder and the counterions and co-ions are modeled as charged hard spheres of equal diameter. The density functional theory is based on a hybrid approach where the hard-sphere contribution to the one-particle correlation function is evaluated nonperturbatively and the ionic contribution to the one-particle correlation function is evaluated perturbatively. The advantage of the approach is that analytical expressions are available for all the correlation functions. The calculated single ion preferential interaction coefficients, excess free energy, and activity coefficients show a nonmonotonic variation as a function of polyion charge in the presence of divalent ions. These properties display considerable departure from the predictions of the nonlinear Poisson-Boltzmann (NLPB) equation, with qualitative differences in some cases, which may be attributed to correlation effects neglected in the NLPB theory.

INTRODUCTION

The interactions of salt ions with polymeric and oligomeric nucleic acids in solution have large and distinctive effects on ionic distributions and thermodynamic coefficients, and thus on equilibrium processes such as conformational transitions and binding interactions (Beveridge and Lavery, 1991). For example, the equilibrium and kinetics of processes involving DNA show apparent equilibrium coefficients that manifest large salt dependencies (Clementi and Sarma, 1983). The counterions in the immediate vicinity of a highly charged cylindrical ion (such as DNA) are believed to be electrostatically associated rather than immobilized at specific sites. The purpose of this paper is to evaluate the thermodynamic consequences of this electrostatic association (or nonuniform counterion distribution) using density functional theory.

Advances in the last few decades have made possible the calculation of thermodynamic coefficients such as the Donnan coefficient, activity coefficient, and osmotic coefficient. Most studies are based on two well-known models: the Poisson-Boltzmann (PB) cell model (Katchalsky, 1975; Stigter, 1975) and the counterion condensation (CC) (Manning, 1979) model. Marcus (1955) used the PB cell model of dilute polyelectrolyte solutions to obtain general expressions for the polyelectrolyte contribution to the mean activity coefficient of added electrolyte, and for the osmotic coefficient of the solvent. Many other studies have used these results to calculate the colligative properties from the PB cell model (Gross and Strauss, 1966; Alexandrowicz and Katchalsky, 1963). Manning (1979) applied the McMillan-

Mayer theory of electrolyte solutions to obtain the dominant contribution to the excess electrostatic free energy arising from charged rod-like polyions in very dilute solutions. From this expression for the free energy (referred to as the "Debye-Hückel" free energy), which exhibits a logarithmic dependence on ionic strength, he obtained a set of limiting-law expressions for the colligative properties of weakly charged cylindrical polyions. For polyions whose axial charge density exceeded a certain critical value, Manning modified the Debye-Hückel excess free energy by introducing the hypothesis of counterion condensation, and derived a second set of limiting law expressions.

Detailed theoretical comparisons between CC and PB theories as applied to ion distributions and thermodynamic properties in different concentration regimes have been reviewed by Anderson and Record (1982). They have also carried out a detailed thermodynamic analysis of effects of salt in ligand-nucleic acid interactions on the basis of preferential interaction coefficients (Anderson and Record, 1995). Although they carried out a number of studies for the ion distributions around DNA, their studies do not shed much light on thermodynamic consequences of salt/DNA interactions. Grand canonical Monte Carlo (GCMC) simulations for calculating the colligative properties of polyelectrolyte solution have also been carried out (Vlachy and Haymet, 1986; Mills et al., 1986) and the results compared to predictions of the PB cell model.

An understanding of the thermodynamic and mechanistic aspects of protein-nucleic acid interactions is central to the elucidation of the molecular basis of the control of gene expression. Structural analyses of protein-DNA complexes suggest that binding free energies depends on direct interactions involving both polar and nonpolar contacts and indirect interactions involving conformation-dependent effects on long-range forces such as electrostatic and salt effects (Harrison and Aggarwal, 1990). The binding free energy of protein-DNA complexes depends strongly on salt

Received for publication 12 July 1999 and in final form 27 October 1999.

Address reprint requests to Dr. Arun Yethiraj, Dept. of Chemistry, University of Wisconsin, 1101 University Ave., Madison, WI 53706. Tel.: 608-262-0258; Fax: 608-262-9918; E-mail: yethiraj@chem.wisc.edu.

© 2000 by the Biophysical Society

0006-3495/00/02/699/08 \$2.00

concentration (Record et al., 1991) and the linkage between electrolyte activity and binding is related to the energies of interaction of the ion-polyion system (Misra et al., 1994b).

There have been several attempts to calculate the free energy of a polyion-salt system from first principles. The first successful calculation of the interaction free energy of the ion-polyion system for the PB cell model was carried out by Lifson and Katchalsky (1954) and independently by Marcus (1955). Manning (1969) calculated the electrostatic contribution to the free energy of the ion-polyion system in the limit of low salt concentrations and compared it to the predictions of Gross and Strauss (1966). Record et al. (1976) modified the expression of free energy predicted by CC theory and applied it to ion effects on ligand-DNA interactions. Recently, Sharp and Honig (1990) (SH) investigated finite difference solutions to the linearized PB, non-linear PB (NLPB), and cell model PB by way of an undetermined multiplier in the Euler-Lagrange equation, and calculated the total electrostatic energy of an ion-polyion system. This procedure has been successfully applied for the calculation of salt effects in ligand-DNA binding (Misra et al., 1994b) and protein-DNA interactions (Misra et al., 1994a). The calculation of electrostatic free energy through the procedure of SH (Sharp and Honig, 1990) and its subsequent application (Misra et al., 1994a,b) is regarded as a breakthrough in terms of calculation of binding constants of reactions involving DNA and salt.

The Sharp and Honig (1990) theory, its success notwithstanding, has two drawbacks: it does not incorporate bulk ion-ion correlations and it does not carry out an overall minimization of the free energy. The effects of bulk ion-ion correlations can be important when the polyion charge density is high, divalent salts are present, or concentrated salt solutions are considered. These shortcomings of the theory can be overcome without significantly increasing the computational requirements via density functional theory (DFT; Hohenberg and Kohn, 1964).

Density functional theory starts with an approximate expression for the free energy as a function of the density distributions of the small ions in an external field (which is the polyion). A minimization of the free energy then gives the density distributions and the minimal free energy. Our objective in the present work is to introduce a partially perturbative DFT approach for the polyion-salt system. The hard sphere contribution to the excess free energy is calculated through a nonperturbative weighted density approximation (WDA) and the electrical contribution is calculated by perturbation with respect to the uniform fluid. The detailed procedure and the results for the ion density profiles and the mean electrostatic potential profiles have been reported earlier (Patra and Yethiraj, 1999) where we showed the theory was accurate when compared with computer simulations for the ion distributions around charged cylinders. In this paper we calculate the total electrostatic free energy for the ion-polyion system in the presence of mono-

valent and divalent counterions. The colligative properties such as preferential interaction coefficients, osmotic coefficients, and activity coefficients are obtained from the free energy and density distributions.

For monovalent salts, the predictions of the DFT and NLPB theory are qualitatively similar, but significant differences are observed in the presence of divalent salts. The accuracy of the DFT is established by comparing it to “exact” computer simulation results for the preferential interaction coefficient. Even for monovalent salts, we find that the NLPB theory is accurate only because the hard sphere contribution in the DFT almost exactly cancels the electrostatic correlation contribution. With divalent ions present, the predictions of the two theories can be qualitatively different. For 2:1 and 2:2 salts, the sign of the free energy is different in the two theories when the polyion is highly charged. This difference can be attributed to the fact that correlation effects become important and the density distributions predicted by the two approaches are vastly different.

The rest of this paper is organized as follows. The theory is outlined in the next section, the results are presented in the third section, and some concluding remarks are offered in the last section.

THEORETICAL FORMULATION

Molecular model

The polyion is modeled as an infinite, isolated, rigid cylinder bearing a uniform axial charge density given by

$$\xi = \frac{\beta_0 e^2}{\epsilon b} \quad (1)$$

where e is the charge of an electron, b is the inverse of linear charge density, $\beta_0 = (k_B T)^{-1}$, k_B is Boltzmann's constant, T is the temperature, and ϵ is the dielectric constant of the pure solvent (which is modeled as a uniform dielectric continuum). In this work we set $\epsilon = 78.358$, $T = 298.15$ K, and $b = 1.7$ Å. The small ions (with α denoting the species) are modeled as charged hard spheres of equal diameter, $d_\alpha = 4$ Å, and charge q_α . The polyion radius is $R = 8$ Å, i.e., the distance of closest approach of the small ions is 10 Å. This is a simple (though popular) model and cannot easily be linked to a real system. Following previous work, we refer to monovalent and divalent cations as Na^+ and Mg^{2+} , respectively, and monovalent anions as Cl^- . We emphasize that this nomenclature is based on the charge of the ions alone. All other differences between these ions, such as size, dispersion interactions, interactions with solvent, etc., which could have important contributions to the thermodynamics, are not considered.

Density functional theory

In density functional theory one starts with an expression for the grand free energy, Ω , as a functional of the singlet density profiles, $\rho_\alpha(\mathbf{r})$, of each of the species, α . At equilibrium the grand free energy is minimal with respect to variations in the density profiles, i.e.,

$$\frac{\delta \Omega}{\delta \rho_\alpha(\mathbf{r})} = 0 \quad (2)$$

for each α and this condition is used to determine the density profiles and the free energy.

The grand potential functional is related to the Helmholtz free energy functional through a Legendre transform,

$$\Omega[\{\rho_\alpha\}] = F[\{\rho_\alpha\}] + \sum_\alpha \int d\mathbf{r} [u_\alpha(\mathbf{r}) - \mu_\alpha] \rho_\alpha(\mathbf{r}), \quad (3)$$

where $u_\alpha(\mathbf{r})$ is the external field (due to the polyion) acting on the atoms of species α , μ_α is the chemical potential of the α th component, and $\{\rho_\alpha\}$ is the set of all density profiles.

The main approximation in density functional theory is the expression for $F[\{\rho_\alpha\}]$. Without loss of generality, this functional may be decomposed into four parts:

$$\begin{aligned} F[\{\rho_\alpha\}] = & k_B T \sum_\alpha \int d\mathbf{r} \rho_\alpha(\mathbf{r}) \{ \ln[\rho_\alpha(\mathbf{r}) \lambda_\alpha^3] - 1 \} \\ & + F_{\text{ex}}^{\text{hs}}[\{\rho_\alpha\}] \\ & + \frac{1}{2} \iint d\mathbf{r}_1 d\mathbf{r}_2 \sum_{\alpha\beta} q_\alpha q_\beta \frac{\rho_\alpha(\mathbf{r}_1) \rho_\beta(\mathbf{r}_2)}{|\mathbf{r}_1 - \mathbf{r}_2|} \\ & + F_{\text{ex}}^{\text{el}}[\{\rho_\alpha\}], \end{aligned} \quad (4)$$

where λ_α is the de Broglie wavelength of the α th component and q_α is the valence of species α . The first term is the exact ideal gas contribution, the second term is the hard sphere contribution, the third term is the direct Coulomb contribution in the mean-field approximation, and the fourth term is the residual electrostatic contribution. The last term includes the coupling of Coulombic and hard sphere interactions, but excludes the direct Coulomb part included in the third term. The main approximations in the theory are expressions for $F_{\text{ex}}^{\text{hs}}$ and $F_{\text{ex}}^{\text{el}}$ which describe liquid-like correlations. These terms are set equal to zero in the NLPB approximation.

In this work we are largely interested in the difference between the free energy in the presence of the polyion from that of a uniform fluid at the same chemical potential. If the corresponding bulk densities are denoted ρ_α^0 , then the grand free energy functional may be written as

$$\begin{aligned} \Omega[\{\rho_\alpha\}] = & \Omega[\{\rho_\alpha^0\}] \\ & + \frac{1}{\beta_0} \sum_\alpha \int d\mathbf{r} \left[\rho_\alpha(\mathbf{r}) \ln \frac{\rho_\alpha(\mathbf{r})}{\rho_\alpha^0} - \rho_\alpha(\mathbf{r}) + \rho_\alpha^0 \right] \\ & + \sum_\alpha \int d\mathbf{r} \rho_\alpha(\mathbf{r}) [u_\alpha^{\text{hs}}(\mathbf{r}) + q_\alpha \psi(\mathbf{r})] \\ & + F_{\text{ex}}^{\text{hs}}[\{\rho_\alpha\}] - F_{\text{ex}}^{\text{hs}}[\{\rho_\alpha^0\}] \\ & + F_{\text{ex}}^{\text{el}}[\{\rho_\alpha\}] - F_{\text{ex}}^{\text{el}}[\{\rho_\alpha^0\}] \end{aligned} \quad (5)$$

where $\psi(\mathbf{r})$ is the mean electrostatic potential at position \mathbf{r} and is the solution to the nonlinear PB equation.

The true equilibrium density distribution of each component is obtained from a minimization of the grand free energy with respect to the density

profiles, which gives,

$$\begin{aligned} \rho_\alpha(x) = & \rho_\alpha^0 \exp\{-\beta_0 q_\alpha \psi(x) \\ & + c_\alpha^{(1)\text{hs}}(x; [\{\rho_\alpha\}]) - c_\alpha^{(1)\text{hs}}([\{\rho_\alpha^0\}]) \\ & + c_\alpha^{(1)\text{el}}(x; [\{\rho_\alpha\}]) - c_\alpha^{(1)\text{el}}([\{\rho_\alpha^0\}]) \} \end{aligned} \quad (6)$$

for $x > (R + d_\alpha/2)$ and zero otherwise, x is measured along the radial direction, and the $c_\alpha^{(1)}(x; [\{\rho(x)\}])$ are the first-order correlation functions for the nonuniform system. Following Patra and Ghosh (1993, 1994, 1997) $c_\alpha^{(1)\text{hs}}(x; [\{\rho_\alpha\}])$ is evaluated using a weighted density approximation (Denton and Ashcroft, 1991) and $c_\alpha^{(1)\text{el}}(x; [\{\rho_\alpha\}])$ is evaluated perturbatively. Explicit analytical expressions for these functions are available elsewhere (Patra and Yethiraj, 1999). Once the equilibrium density distribution and the mean electrostatic potential are determined, the total electrostatic free energy and its different contributions can be calculated with the bulk fluid as the reference state (Sharp and Honig, 1990).

In the Results section we discuss various contributions to the solvation Helmholtz free energy, i.e., the free energy of the polyion-electrolyte system minus that of the electrolyte solution without the polyion. These contributions are defined as

$$F_\psi = \sum_\alpha \int d\mathbf{r} \rho_\alpha(\mathbf{r}) [u_\alpha^{\text{hs}}(\mathbf{r}) + q_\alpha \psi(\mathbf{r})], \quad (7)$$

$$F_{\text{id}} = \frac{1}{\beta_0} \sum_\alpha \int d\mathbf{r} \left[\rho_\alpha(\mathbf{r}) \ln \frac{\rho_\alpha(\mathbf{r})}{\rho_\alpha^0} - \rho_\alpha(\mathbf{r}) + \rho_\alpha^0 \right], \quad (8)$$

$$F_{\text{ex}}^{\text{hs}} = F_{\text{ex}}^{\text{hs}}[\{\rho_\alpha\}] - F_{\text{ex}}^{\text{hs}}[\{\rho_\alpha^0\}] \quad (9)$$

$$F_{\text{ex}}^{\text{el}} = F_{\text{ex}}^{\text{el}}[\{\rho_\alpha\}] - F_{\text{ex}}^{\text{el}}[\{\rho_\alpha^0\}]. \quad (10)$$

Other thermodynamic quantities of interest are defined in the usual fashion. The preferential interaction coefficient $\Gamma_{3,2}$ provides the thermodynamic characterization of the interactions of a solute or co-solute (component 3) with a relatively larger solute (component 2) present at sufficiently high dilution in the solvent (component 1). The excess solute 3 may be a nonelectrolyte or an electrolyte; the dilute solute 2 may be oligomeric or polymeric, charged or uncharged. According to the usual definition (Eisenberg, 1976)

$$\Gamma_{3,2} = \left(\frac{\partial c_3}{\partial c_2} \right)_{T, \mu_1, \mu_3} \quad (11)$$

where c_3 is the molar concentration of component 3 and c_2 is the molar concentration of component 2. These coefficients can sometimes be measured by means of dialysis equilibrium experiments (Gross and Strauss, 1966). When c_2 is low enough, $\Gamma_{3,2}$ is equal to the experimental dialysis coefficient, defined as

$$\lim_{c_2 \rightarrow 0} \equiv \Gamma_{3,2}^0 = \lim_{c_2 \rightarrow 0} \frac{c_3 - c'_3}{c_2} \quad (12)$$

where c'_3 is the solute molarity in the dialysis solution. In the present case solute 3 is a mixed salt and the individual (but not independent) preferential interactions of each ion with the polyion is characterized by a single-ion preferential interaction coefficient (Lippincott, 1988) defined as the accumulation of counterions or the exclusion of co-ions. Thus in the present

case,

$$\Gamma_{\alpha} = 2\pi b \int_0^{\infty} dx' x' [\rho_{\alpha}(x') - \rho_{\alpha}^0]. \quad (13)$$

The activity coefficient, γ_{α} , of small ions is obtained from the density distributions (Marcus, 1955) using

$$\gamma_{\alpha} = \rho_{\alpha}^0 \left[\frac{2}{R_M^2} \int_0^{R_M} x \rho_{\alpha}(x) dx \right]^{-1}, \quad (14)$$

where R_M is the maximum radial distance in the calculations and is chosen large enough that the density distributions are uniform at this position.

RESULTS AND DISCUSSION

The density functional theory is in good agreement with computer simulations for the density distributions of small ions around polyions, as has been demonstrated earlier (Patra and Yethiraj, 1999). The thermodynamic quantity that is most directly related to the density distribution is the preferential interaction coefficient. Small ion correlations are significant and the DFT predictions are closer to the simulation results than the PB predictions. This can be seen in Fig. 1, which compares theoretical predictions for Γ_{α} in mixed salts to computer simulations (Ni et al., 1999) for 1:1 (NaCl) salt concentrations of 16 mM, 72 mM, and 239 mM as a function of added MgCl_2 concentration. The polyion charge is characterized by a value of $\xi = 4.2$, which is appropriate for DNA. Solid lines are predictions of the density functional theory and dashed lines are predictions of the NLPB theory. For a fixed value of Mg^{2+} concentration, increasing NaCl concentration results in increasing Γ_{Na} and decreasing Γ_{Mg} . Similarly, increasing the Mg^{2+} concentra-

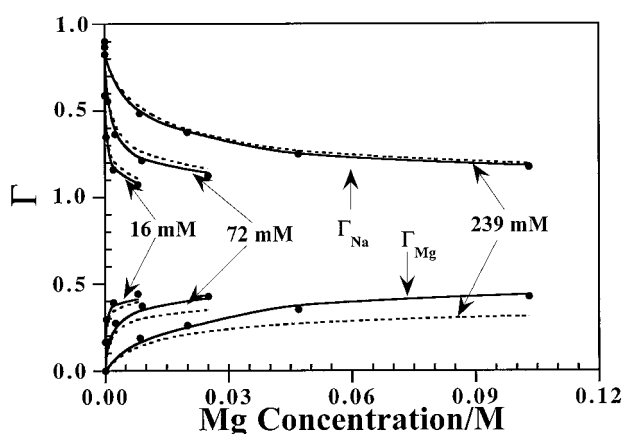


FIGURE 1 Comparison of theoretical predictions for the preferential interaction coefficient to Monte Carlo simulations (Ni et al., 1999) for various NaCl concentrations (as marked) as a function of added MgCl_2 concentration. Symbols are simulation results and lines are predictions of the density functional theory (—) and nonlinear Poisson-Boltzmann theory (---).

tion results in increasing Γ_{Mg} and decreasing Γ_{Na} . Both theories are in good agreement with the simulations, although the density functional theory is in quantitatively closer agreement with the simulations than the NLPB, especially for Γ_{Mg} at high concentrations.

The predictions of the DFT and NLPB theories for the free energy are qualitatively similar for monovalent salts, but distinctive and sometimes large differences between the theories are observed when divalent ions are present. Fig. 2, *a–c* depict the DFT and NLPB predictions for the negative of the solvation free energy as a function of the charge per unit b for 1:1, 2:1, and 2:2 electrolytes, respectively, and for three salt concentrations in each case. For the 1:1 salt (Fig. 2 *a*) both theories predict that the free energy decreases monotonically with increasing charge on the polyion. Except at high values of the charge, the predictions of the two approaches are quantitatively quite similar.

The predictions of the two theories for the free energy are vastly different when divalent ions are present. For 2:1 salts (Fig. 2 *b*) the total free energy predicted by DFT and NLPB are of opposite sign for charges >2 per b . At the highest value of charge per b shown, the difference between the two theories is $\sim 40 k_B T$. This emphasizes the importance of correlation effects in highly charged systems that are excluded in the NLPB theory. At the highest concentration depicted (239 mM) the free energy shows a minimum as a function of the charge, which occurs at different values of the charge in the two theories. The predictions for 2:2 salts (Fig. 2 *c*) are qualitatively similar to those for the 2:1 salt, although there are numerical differences.

More insight into the performance of the theories can be obtained by looking at the ideal gas, bare electrostatic, hard sphere, and electrical contributions to free energy. Recall that the last two terms are set to zero in the NLPB theory. Fig. 3, *a* and *b* depict these contributions, viz. F_{id} , F_{ψ} , $F_{\text{ex}}^{\text{hs}}$, and $F_{\text{ex}}^{\text{el}}$ for 16 mM 1:1 and 2:2 salts, respectively.

For monovalent salts the predictions of the two theories for the free energies are similar, in part because the hard sphere and electrical contributions in the DFT tend to cancel each other. If we look at the various contributions, F_{id} increases up to a certain charge and then decreases in both DFT and PB, although the change is rather small, indicating the constancy of this energy with increase of charge. Also, the difference between the two theories for this quantity is rather small. F_{ψ} decreases continuously as the charge is increased and again, the difference between the DFT and PB predictions is rather small. $F_{\text{ex}}^{\text{hs}}$ increases continuously with increasing charge, whereas $F_{\text{ex}}^{\text{el}}$ decreases by almost the same amount. These two contributions, both of which are neglected in the NLPB theory, almost exactly cancel each other. The accuracy of the NLPB theory may thus be viewed as being caused by a fortuitous cancellation of errors.

The large differences between the predictions of the DFT and NLPB in the presence of divalent salts arises from the differences in the F_{ψ} contribution in the two approaches. In

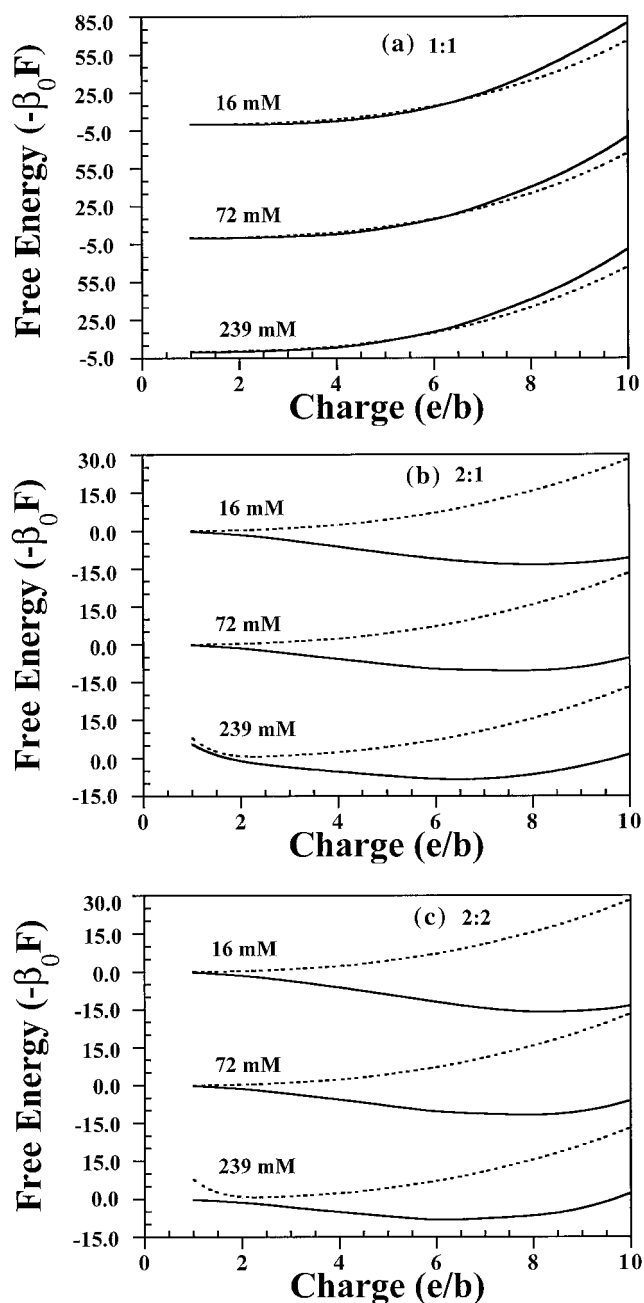


FIGURE 2 Free energy of solvation as a function of charge on the polyelectrolyte for various salt concentrations (as marked) for (a) 1:1 salt, (b) 2:1 salt, and (c) 2:2 salts. Lines are predictions of the DFT (—) and NLPB (---) theories. Note that the negative of the free energy is plotted on the ordinate.

Fig. 3 *b*, the ideal gas contributions from the two approaches are very similar. In fact, the ideal gas contribution in divalent salts is very similar to that in monovalent salts at the same concentration. Again, $F_{\text{ex}}^{\text{hs}}$ and $F_{\text{ex}}^{\text{el}}$ are large and of opposite sign and tend to cancel each other. This cancellation, however, is not as complete as it is for the 1:1 salt. The large difference in the free energies comes from the F_{ψ}

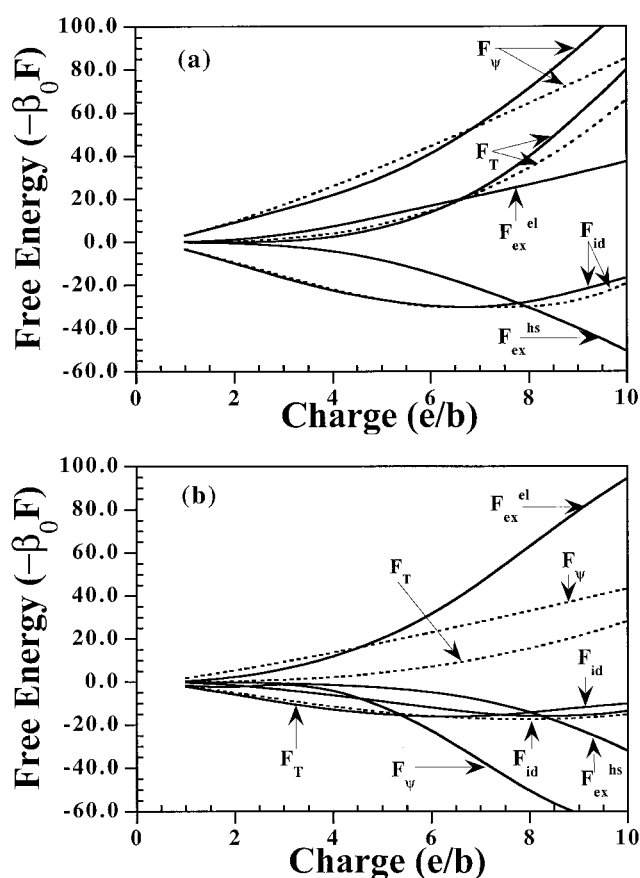


FIGURE 3 Various contributions to the free energy from DFT (—) and NLPB (---) theories for (a) 16 mM 1:1 salt, and (b) 16 mM 2:2 salt.

term, which is negative in the NLPB and positive in the DFT. Note that the form of the F_{ψ} contribution is identical in the two approaches; the density distributions predicted by the two approaches are different. The density distributions for 16 mM 2:1 and 2:2 salts are depicted in Fig. 4. The DFT predicts a significant accumulation of counterions and co-ions near the polyanion, which is not observed in the NLPB theory. In general, dramatic changes in the density distributions are observed in the DFT approach for high charges that are missing from the NLPB theory (Patra and Yethiraj, 1999). The DFT predicts a charge inversion at these high charge densities, i.e., the mean electrostatic potential turns to be positive for the negative polyanion. This charge inversion is missed by the NLPB theory because it does not include correlation effects, and the theory therefore always predicts negative values for F_{ψ} .

Fig. 5 depicts the activity coefficient of the divalent counterions for a 72-mM NaCl as a function of added MgCl_2 concentration. Again, the DFT predictions display a large departure from those of the NLPB theory. A direct test is not possible because there are no computer simulation results for these thermodynamic properties. In previous work (Patra and Yethiraj, 1999) we compared the theoretic-

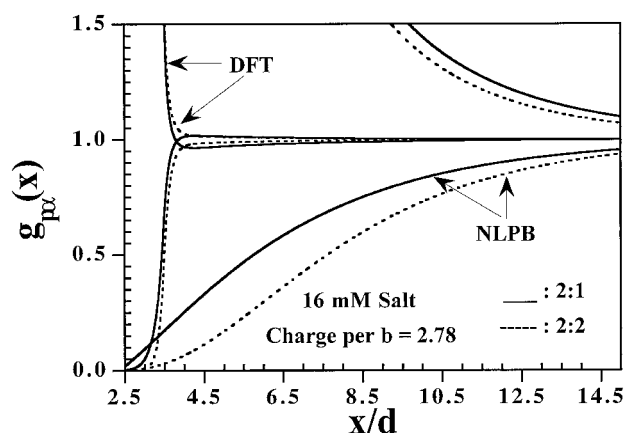


FIGURE 4 Co-ion and counterion distributions around the polyion normalized to the bulk value for 16 mM 2:1 (—) and 2:2 (---) salts from the DFT and NLPB theories (as marked) for charge per b of 2.78.

cal predictions for density distributions to computer simulations and showed that the DFT was in much closer agreement with simulations than the NLPB theory. This is also seen in Fig. 1, where the DFT is in closer agreement with simulations for the preferential interaction coefficients than the NLPB theory. We therefore expect the DFT predictions of the thermodynamics to be more accurate than the NLPB approach.

CONCLUDING REMARKS

We present a density functional approach for the density distributions, total electrostatic free energy, and the associated colligative properties, viz. the preferential interaction coefficient, the activity coefficients, and the osmotic coefficients of polyelectrolyte solutions. The formalism is partially perturbative in the sense that it treats the hard sphere correlations with a weighted density approximation and

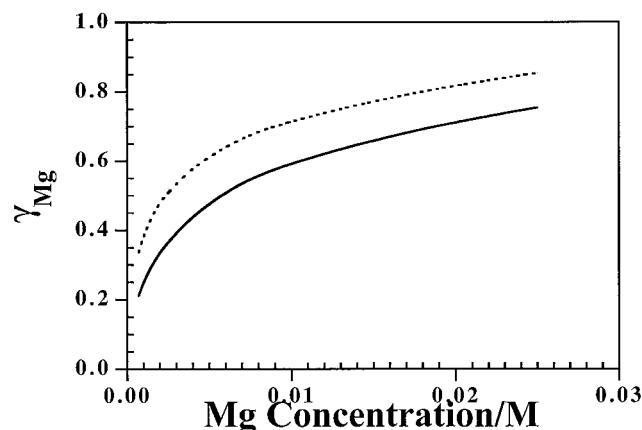


FIGURE 5 Activity coefficient for a mixed salt as a function of added MgCl_2 concentration for a 72-mM NaCl salt with $\xi = 4.2$. Lines are predictions of DFT (—) and NLPB (---) theories.

treats the electrical contribution with a perturbation with respect to the uniform fluid. The total electrostatic free energy is calculated with respect to a reference fluid, which is taken as the bulk salt without the polyion. This theory has been previously shown to be accurate for the density distributions in polyelectrolyte solutions (Patra and Yethiraj, 1999).

For a pure 1:1 salt, the excess hard sphere and the electrical contribution to the free energy almost cancel each other and the DFT results for the total electrostatic free energy are almost identical to the nonlinear Poisson-Boltzmann (NLPB) theory, even up to a charge of 10 per b . This result has implications in ion distributions and preferential interaction coefficients, for which case the NLPB predictions are comparable to those of the DFT when compared to Monte Carlo simulations (Patra and Yethiraj, 1999).

When divalent counterions are present, two important effects emerge which are absent in 1:1 salt. First of all, the DFT prediction for the bare electrostatic contribution, F_{ψ} , becomes positive for high values of charge because of a charge inversion effect. The NLPB always predicts a negative value for this quantity. Second, the cancellation between the hard sphere and electrical contribution for the free energy is not as complete as in the 1:1 case. The result is that for high values of the charge per b , the DFT and NLPB theories predict free energies of opposite sign. Interestingly, for a comparable concentration and charge density at the polyion, the total electrostatic free energy is lower for a 2:2 salt, and the F_{ψ} is lower for a 2:1 salt because for a 2:2 salt the bulk attraction is more than the polyion-ion attraction in the vicinity of the polyion, whereas the opposite is true for the 2:1 salt.

The polyelectrolyte solution is nonideal in the presence of salt, as can be seen from the preferential interaction coefficient profiles. Contrary to the normal salt case, the nonideality of the polyelectrolyte solution decreases with increasing salt concentration. The preferential interaction coefficients are very sensitive to the divalent ion concentration and almost insensitive to the monovalent ion concentration. At a higher divalent ion concentration, the NLPB results are in much poorer agreement with simulations than the DFT predictions because the NLPB does not take small ion correlations into account.

The increasingly ideal behavior with increases in overall salt concentration is also observed in the calculation of other colligative properties, viz. activity coefficients and the osmotic coefficients that tend to unity as the overall concentration is increased. Again, for a pure 1:1 salt, both DFT and NLPB are quite similar, but significant differences are seen in the presence of divalent ions.

The density distributions and the associated thermodynamic data support the behavior of the ion-polyion interaction as calculated from the total electrostatic free energy. In essence, all the results are complementary to one another and can explain the interaction of an ion-polyion system

only through the electrostatic effects. That the small ion correlations are really important can be very clearly seen in the case of multivalent ions, where at a comparable concentration and the polyion charge density, the charge inversion is seen for a 2:1 salt and not in a 2:2 salt.

It is certainly possible to investigate more complex models of the polyions and ions in solution. The incorporation of chemical details in the molecular model for the polyion is conceptually trivial because this only alters the external field in the free energy functional. The main challenge is a numerical one: in this case we no longer have cylindrical symmetry and the density distributions have to be calculated on a three-dimensional grid. Such calculations are routinely carried out using the NLPB equation (Misra et al., 1994a,b), and should be possible with the DFT as well. Similarly, it is possible to incorporate more realistic repulsive and dispersion interactions into the ion-ion potentials with more numerical work. In this case one would implement the DFT without change, but with the full intermolecular potential replaced with an optimally determined hard core plus tail potential, using standard liquid state methods. The only difference from the present work is that the direct correlation functions would have to be calculated numerically instead of analytically.

It is also possible to include the solvent (water) as a third component in the liquid if the interactions are pairwise decomposable and a theory for the bulk uniform fluid is available. In this case the presence of internal degrees of freedom in the molecular solvent makes this extension more complicated than the other extensions discussed above. We have developed a density functional theory for polymers at surfaces where these internal degrees of freedom are incorporated exactly (Yethiraj and Woodward, 1995; Yethiraj, 1998), and the density profiles of the molecular liquid are obtained from the simulation of a single molecule in a self-consistently determined field. The implementation of the theory is similar to what is done here except that the equations to be solved involve a single molecule simulation. Briefly, in the DFT we start with a guess for the density profiles, calculate the correlation functions, and then obtain the next guess for the density profiles from Eq. 6. This procedure is continued to convergence. If one of the components is molecular in nature, e.g., water, then the calculation of the new density profiles entails the simulation of a single molecule in a self-consistent field due to the rest of the fluid. This is the computationally demanding step for polymers, but is not particularly difficult for water. The real difficulty, of course, is that we are not aware of any accurate theory for the correlation functions in bulk water, and this is required as input into the DFT.

In summary, we have presented a theory which allows one to include small ion correlations in a relatively simple fashion. This is possible partly because the correlation functions required are available in analytic form, thus making the theory convenient and tractable. We consider the sim-

plest possible case, i.e., a salt solution around a single charged cylinder, and quantify effects due to small ion correlations. It would be useful to verify these predictions using computer simulations.

We gratefully acknowledge support from Sandia National Laboratories, the Sloan Foundation, and the National Science Foundation [through grant numbers CHE 9732604 (to A.Y.) and CHE 952207 (to the Department of Chemistry)].

REFERENCES

- Alexandrowicz, Z., and A. Katchalsky. 1963. Colligative properties of polyelectrolyte solutions in excess of salt. *J. Polym. Sci.* 1:3231–3260.
- Anderson, C. F., and M. T. Record, Jr. 1982. Polyelectrolyte theories and their application to DNA. *Annu. Rev. Phys. Chem.* 33:191–222.
- Anderson, C. F., and M. T. Record, Jr. 1995. Salt nucleic acid interactions. *Annu. Rev. Phys. Chem.* 46:657–700.
- Beveridge, D. L., and R. Lavery, editors. 1991. *Theoretical Biochemistry and Molecular Biophysics*. Adenine, New York.
- Clementi, E., and R. H. Sarma, editors. 1983. *Structure and Dynamics: Nucleic Acids and Proteins*. Adenine, New York.
- Denton, A. R., and N. W. Ashcroft. 1991. Weighted density functional theory of nonuniform fluid mixtures—application to the structure of binary hard sphere mixtures near a hard wall. *Phys. Rev. A* 44: 8242–8248.
- Eisenberg, H. 1976. *Biological Macromolecules and Polyelectrolytes in Solution*. Clarendon, Oxford.
- Gross, L. M., and U. P. Strauss. 1966. *Chemical Physics of Ionic Solutions*. B. E. Conway and R. G. Barradas, editors. Wiley, New York.
- Harrison, S. C., and A. K. Aggarwal. 1990. DNA recognition by proteins with the helix-turn-helix motif. *Annu. Rev. Biochem.* 59:933–969.
- Hohenberg, P., and W. Kohn. 1964. Inhomogeneous electron gases. *Phys. Rev. B* 136:864–871.
- Katchalsky, A. 1975. Polyelectrolytes. *Pure and Applied Chemistry*. 26: 327–373.
- Lifson, S., and A. Katchalsky. 1954. The electrostatic free energy of polyelectrolyte solutions. II. Fully stretched macromolecules. *J. Polym. Sci.* 13:43–55.
- Lippincott, T., editor. 1988. *Sourcebook for Physical Chemistry Instructors*. American Chemical Society, Washington, DC.
- Manning, G. S. 1969. Limiting laws and counterion condensation in polyelectrolyte solutions. I. Colligative properties. *J. Chem. Phys.* 51: 924–933.
- Manning, G. S. 1979. Counterion binding in polyelectrolyte theory. *Accounts of Chemical Research*. 12:443–449.
- Marcus, R. H. 1955. Calculation of thermodynamic properties of polyelectrolytes. *J. Chem. Phys.* 23:1057–1078.
- Mills, P., C. F. Anderson, and M. T. Record, Jr. 1986. Grand canonical Monte Carlo calculations of thermodynamic coefficients for a primitive model of DNA-salt solutions. *J. Phys. Chem.* 90:6541–6548.
- Misra, V. K., J. L. Hecht, K. A. Sharp, R. A. Friedman, and B. Honig. 1994a. Salt effects on protein-DNA interactions—the λ -CI repressor and *ecori* endonuclease. *J. Mol. Biol.* 238:264–280.
- Misra, V. K., K. A. Sharp, R. A. Friedman, and B. Honig. 1994b. Salt effects on ligand-DNA binding-minor groove binding antibiotics. *J. Mol. Biol.* 238:245–263.
- Ni, H. H., C. F. Anderson, and M. T. Record, Jr. 1999. Quantifying the thermodynamic consequences of cation (M^{2+} , M^{+}) accumulation and anion (X^{-}) exclusion in mixed salt solutions of polyanionic DNA using Monte Carlo and Poisson-Boltzmann calculations of ion-polyion preferential interaction coefficients. *J. Phys. Chem.* 103:3489–3504.

- Patra, C. N., and S. K. Ghosh. 1993. Weighted density functional theory of non-uniform ionic fluids—application to electrical double layers. *Phys. Rev. E*. 47:4088–4097.
- Patra, C. N., and S. K. Ghosh. 1994. A nonlocal density functional theory of electric double layer-symmetrical electrolytes. *J. Chem. Phys.* 100: 5219–5229.
- Patra, C. N., and S. K. Ghosh. 1997. Structure of inhomogeneous dipolar fluids: a density functional approach. *J. Chem. Phys.* 106:2752–2761.
- Patra, C. N., and A. Yethiraj. 1999. Density functional theory for the distribution of small ions around charged cylinders. *J. Phys. Chem.* 103:6080–6087.
- Record, M. T., Jr., J. H. Ha, and M. A. Fisher. 1991. Analysis of equilibrium and kinetic measurements to determine thermodynamic origins of stability and specificity and mechanism of formation of site-specific complexes between proteins and helical DNA. *Methods Enzymol.* 208: 291–342.
- Record, M. T., Jr., T. M. Lohman, and P. De Haseth. 1976. Ion effects on ligand-nucleic acid interactions. *J. Mol. Biol.* 107:145–148.
- Sharp, K. A., and B. Honig. 1990. Calculating total electrostatic energies with the nonlinear Poisson-Boltzmann equation. *J. Phys. Chem.* 94: 7684–7692.
- Stigter, D. 1975. The charged colloidal cylinder with a Gouy double layer. *J. Colloid Interface Sci.* 53:296–306.
- Vlachy, V., and A. D. J. Haymet. 1986. A grand canonical Monte Carlo simulation study of polyelectrolyte solutions. *J. Chem. Phys.* 84: 5874–5880.
- Yethiraj, A. 1998. Density functional theory of polymers: a Curtin-Ashcroft-type weighted density approximation. *J. Chem. Phys.* 109: 3269–3275.
- Yethiraj, A., and C. E. Woodward. 1995. Monte Carlo density functional theory of nonuniform polymer melts. *J. Chem. Phys.* 102:5499–5505.